Tracking differentiating neural progenitors in pluripotent cultures using microRNA-regulated lentiviral vectors

Rohit Sachdeva[a], Marie E. Jönsson[a], Jenny Nelander[a], Agnete Kirkeby[a], Carolina Guibentif[a], Bernhard Gentner[b], Luigi Naldini[b], Anders Björklund[a], Malin Parmar[a], and Johan Jakobsson[a,1]

[a]Department of Experimental Medical Sciences, Wallenberg Neuroscience Center, Lund University, 221 84 Lund, Sweden; and [b]San Raffaele-Telethon Institute for Gene Therapy and Vita-Salute San Raffaele University, 201 32 Milan, Italy

Edited by Igor B. Dawid, National Institute of Child Health and Human Development, Bethesda, MD, and approved May 19, 2010 (received for review May 11, 2010)

In this study, we have used a microRNA-regulated lentiviral reporter system to visualize and segregate differentiating neuronal cells in pluripotent cultures. Efficient suppression of transgene expression, specifically in undifferentiated pluripotent cells, was achieved by using a lentiviral vector expressing a fluorescent reporter gene regulated by microRNA-292. Using this strategy, it was possible to track progeny from murine ES, human ES cells, and induced pluripotent stem cells as they differentiated toward the neural lineage. In addition, this strategy was successfully used to FACS purify neuronal progenitors for molecular analysis and transplantation. FACS enrichment reduced tumor formation and increased survival of ES cell–derived neuronal progenitors after transplantation. The properties and versatility of the microRNA-regulated vectors allows broad use of these vectors in stem cell applications.

ES | induced pluripotent stem cells | stem cells | transplantation

Pluripotent stem cells offer an unlimited resource that allows unique access to study the earliest phases of murine and human neuronal development, and neural cells generated from stem cells have the potential to be used for regenerative medicine (1). As a consequence, the development of differentiation protocols that drive pluripotent stem cells toward specific neural fates is valuable, as it will allow studies of neuronal development and disease (1). Although numerous protocols describe efficient neuralization of pluripotent cells, a common feature that they all have is that they result in a heterogeneous cell population (2–5). This limits detailed molecular characterization of specific populations of differentiating cells, and is particularly problematic in transplantation paradigms in which contamination of undifferentiated cells causes overgrowth or rejection of the graft (4, 6, 7).

To track differentiating cell populations, cell-type specific reporter cell lines have been generated by homologous recombination (knock-in) or BAC transgenesis (5, 8). These reporter lines provide robust reporter activity and are, at least in murine cells, increasingly used. Still, the production of BAC and knock-in cell lines is time consuming and remains a technical challenge in regard to human cells, in which only a few successful cases have been described (8, 9). Therefore it seems unlikely that any of these techniques are to be used on a large scale in human cells.

Here we describe an alternative strategy to mark differentiated neural progeny that exploits the endogenous microRNA (miRNA) machinery. miRNAs are small, noncoding, single-stranded RNAs of ~21–23 nucleotides that compose a complex network of gene regulation, the primary role of which is to negatively regulate gene expression by recognizing mRNAs and directing their destruction or inhibiting their use in translation (10). Increasing evidence indicates that miRNAs have distinct expression profiles, including, for example, ES cell–specific and brain-specific miRNAs (10).

The system used in this report is based on lentiviral vectors that encode fluorescent reporters followed by microRNA target (miRT) sequences of an endogenous, pluripotent, specific miRNA. This allows degradation of a fluorescent transgene specifically in pluripotent cells (11, 12). Because the vector exploits the expression pattern of an endogenous miRNAs, it is as robust and reliable as a knock-in or BAC reporter cell line (11, 12). Importantly, the system is advantageous to current technologies because of its simplicity, versatility, and easy transfer from different ES cell lines to induced pluripotent stem (iPS) cell lines or from murine to human cells. Our data provides proof-of-principle of visualization and isolation of neural progenitors using lentiviral vectors expressing a miRNA-regulated fluorescent protein in multiple pluripotent cell systems.

Results

miRNA-Regulated Vectors Efficiently Report GFP Expression in Neural Progenitor Cells. We first investigated the potential of miRNA-regulated vectors to segregate transgene expression between murine neural stem cells (mNS) (13) and murine ES cells (mES). microRNA-292 is highly expressed in mES, but not in mNS (14). We thus constructed a green fluorescent protein (GFP) expressing lentiviral vector that contains target sequences for miR-292 (LV.292T, Fig. 1*A*) in the 3′ untranslated region, and transduced mES and mNS at multiplicities of infection (MOI) of 50 and 10, respectively. The LV.292T vector resulted in high-level GFP expression in mNS, whereas little GFP was detected in mES (Fig. 1 *B–D*). This expression pattern is due to posttranscriptional regulation and can be attributed to the differential expression pattern of miR-292, as transduction with a GFP-vector lacking miR target sites (LV-GFP) to a similar number of vector integrations led to high-level GFP expression in both mES and mNS (Fig. 1 *B* and *E*).

Use of miRNA-Regulated GFP Expression to Track Neural Differentiation of mES Cells. To test whether the loss of miR-292 expression and thus the appearance of GFP in LV.292T-transduced mES (mES.292T) cells could serve as a biomarker for cells committed to the neuronal lineage, we induced neuronal differentiation in mES.292T.

Initially, we used a monolayer protocol described by Ying et al. (5), in which mES.292T cells were plated in a defined medium at low density. The differentiation led to rapid and efficient conversion of mES to neural progenitor cells, and the GFP expression was monitored over time. In undifferentiated cells and at early time points during differentiation (days 1–5) only negligible GFP expression were detected (Fig. 2*A*). However, after 7 d of differen-

Author contributions: R.S., M.E.J., J.N., A.K., A.B., M.P., and J.J. designed research; R.S., M.E.J., J.N., A.K., C.G., and J.J. performed research; B.G. and L.N. contributed new reagents/analytic tools; R.S., M.E.J., J.N., A.K., A.B., M.P., and J.J. analyzed data; and R.S. and J.J. wrote the paper.

The authors declare no conflict of interest.

This article is a PNAS Direct Submission.

[1]To whom correspondence should be addressed. E-mail: johan.jakobsson@med.lu.se.

This article contains supporting information online at www.pnas.org/lookup/suppl/doi:10.1073/pnas.1006568107/-/DCSupplemental.

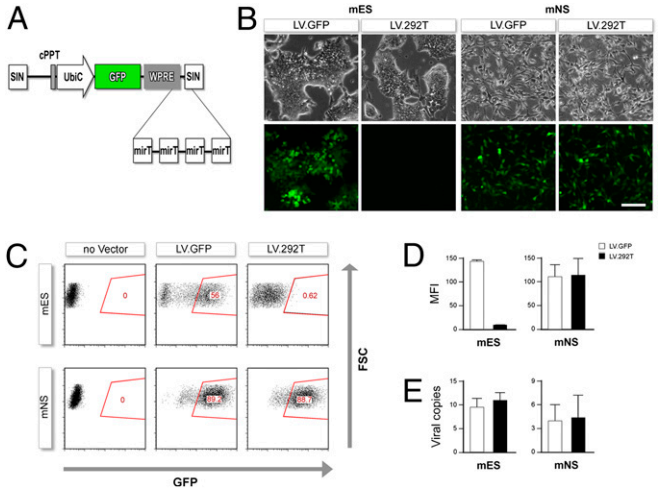

Fig. 1. Mir-292-regulated vectors efficiently separate ES and NS cells. (*A*) Scheme of the proviral form of LV.292T. (*B*) Brightfield and fluorescent microscopy and (*C*) flow cytometry of mES and mNS transduced with either LV.GFP or LV.292T. (*D*) Mean fluorescence intensity (MFI) of the corresponding cultures (n = 3). (*E*) Quantification of viral copies/cell using quantitative PCR from genomic DNA of the cells analyzed in *D* (n = 3). Data are representative of three independent experiments. Error bars represent SD. FSC, forward scatter. (Scale bar, 100 μm.)

tiation, we were able to reproducibly detect GFP expression using flow cytometry and fluorescence microscopy. Initially, GFP was detected at low levels; but as differentiation proceeded, the level of GFP expression increased to the levels observed in in LV.GFP–transduced cells (Fig. 2 *A* and *B*).

The appearance of GFP expression in the differentiating cultures was compared with the temporal induction of the neural

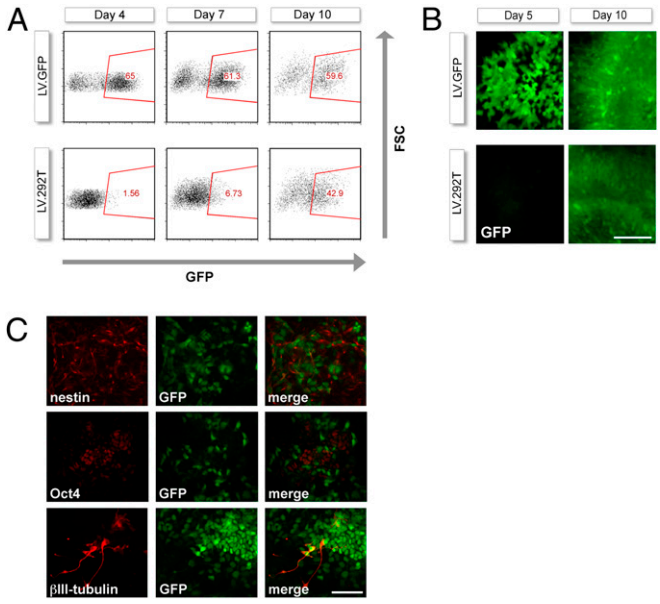

Fig. 2. GFP expression appears when mES differentiate into neurons. (*A*) FACS analysis of mES transduced with either LV.GFP or LV.292T following different time points after initiation of differentiation using monolayer protocol. (*B*) Fluorescent microscopy of live GFP expressing cells 5 and 10 d after the start of monolayer differentiation. (*C*) Fluorescent microscopy of mES differentiated for 7 d using the monolayer protocol. Cultures were immunostained for GFP, nestin, Oct4, and βIII-tubulin. (Scale bar, *B,* 100 μm; *C,* 50 μm.)

progenitor marker nestin and down-regulation of the pluripotency marker gene Oct4 (Figs. S1 and S2). Nestin expression appeared at day 4 and reached high levels after 7 and 10 d of differentiation. Immunostaining confirmed that the majority of nestin-expressing cells colocalized with GFP (Fig. 2*C* and Fig. S1). In contrast, Oct4 expression was gradually down-regulated during the 10-d period; and, as Oct4 expression diminished, GFP expression appeared (Fig. 2*C* and Fig. S2). Even after 10 d of differentiation, a small number of Oct4-expressing cells remained in the cultures; however, immunostaining confirmed that the remaining Oct4-expressing cells did not colabel with GFP (Fig. 2*C* and Fig. S2). After 7 and 10 d of differentiation, a proportion of the GFP-expressing cells also colabeled with the neuronal marker βIII-tubulin (Fig. 2*C*) confirming differentiation into neurons.

It should be added that in addition to visualize neural cells, the LV.292T vector has the potential to track other lineages as demonstrated by transduction of mouse embryonic fibroblasts with LV.292T and differentiation of mES.292T into embryonic bodies in conditions that promote mesoendoderm formation. In both cases high-level GFP expression was detected (Fig. S3).

Cell Sorting Based on miRNA-Regulated GFP Expression Excludes Pluripotent Cells. As a second approach we differentiated mES.292Ts on PA6 stromal feeder cells according to Kawasaki et al. (3). This protocol results in robust neural induction and also specifies a large fraction of the progenitors into dopaminergic neurons. However, PA6-differentiation is asynchronous and large numbers of undifferentiated Oct4-expressing cells remain within the center of the colonies even after extended periods of differentiation, making this protocol challenging to use for molecular analysis and cell transplantation paradigms. As was the case with the monolayer protocol, no GFP-expressing cells could be detected during the first days of differentiation (days 1–4). At day 5, GFP-expressing cells appeared at the edges of the colonies and at later time-points large numbers of GFP-expressing mature neurons could be detected using fluorescent microscopy (Fig. 3*A*). However, cells with immature morphology were present in the center of many colonies also at late time points (days 10–14) and these cells remained GFP-negative (Fig. 3*A*). Immunostainings of fixed cultures confirmed that these immature cells that were GFP negative maintained Oct4 expression (Fig. 3*A*). In contrast, GFP-expressing cells displayed mature morphologies and were negative for Oct4 (Fig. 3*A*).

The appearance of GFP expression when mES.292Ts differentiate opens up the possibility to isolate and purify differentiated progeny. To this end we used FACS sorting to isolate the GFP-expressing cells at day 8 of PA6 differentiation and then immediately analyzed the FACS-purified cells using quantitative immunofluorescence. We found that the GFP-expressing population was enriched for nestin expressing cells, whereas the majority of Oct4 expressing cells were found in the nonsorted fraction (Fig. 3*B* and Fig. S4). We also found that many of the GFP-expressing cells were still proliferating as measured by phosphorylated Histone 3 (pH3) staining that labels cells in the M-phase (Fig. 3*B* and Fig. S4). At day 8, we detected only low numbers of βIII-tubulin neurons but these were also enriched in the GFP expression population (Fig. 3*B* and Fig. S4). In summary, these data demonstrate that the FACS-purified cells represent a population enriched for proliferating nestin-expressing neural progenitors and depleted for undifferentiated pluripotent cells (Fig. 3*B* and Fig. S4). In addition, we performed quantitative RT-PCR on the FACS-purified population that confirmed the results of the immunostainings demonstrating a loss of the pluripotency-related transcripts, Oct4 and Nanog, whereas transcripts associated with neural progenitors cells, such as Nestin and BLBP, were enriched in the GFP-expressing population (Fig. S5). To demonstrate that the GFP-expressing progenitors survive sorting the FACS-purified cells were replated into differentiation conditions. One week after

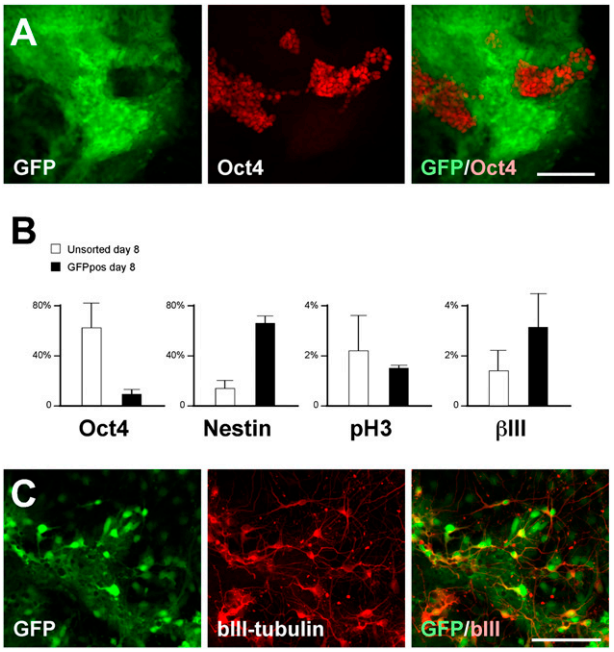

Fig. 3. FACS purification enrichment of nonpluripotent neural progenitor cells. (*A*) Fluorescent microscopy of mES cells differentiated for 8 d using the PA6 protocol. Cultures were immunostained for GFP (green) and Oct4 (red). (*B*) Quantitative immunofluorescent analysis of mES cells differentiated for 8 d using the PA6 protocol and then FACS purifed for GFP-expressing cells. Cells were plated and fixed directly after FACS sort and then immunostained for Oct4, nestin, pH3, and βIII-tubulin, respectively. Representative images are shown in Fig S4. Data are presented as immunopositive cells/DAPI-stained cells (n = 6). (C) Fluorescent microscopy of mES cells after 14 d of differentiation. Cultures were FACS sorted for GFP expression after 8 d of differentiation using the PA6-protocol and then replated into differentiation conditions. Cultures were immunostained for βIII-tubulin and GFP. Error bars represent SD. (Scale bar, 100 μm.)

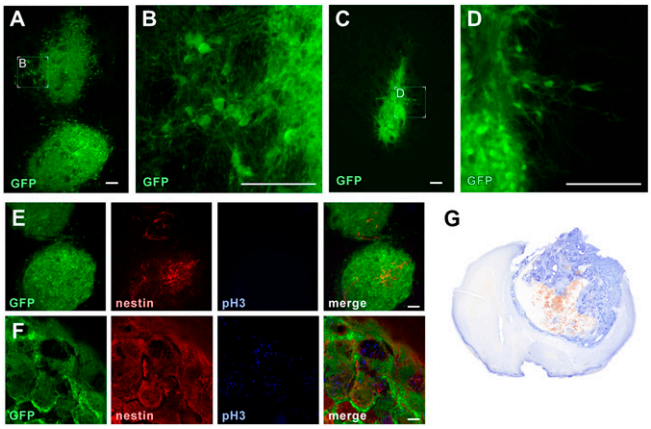

Fig. 4. FACS purification of mESs reduces tumor formation following transplantation into the rodent brain. Confocal microscopy of mES cells grafted into (*A* and *B*) neonatal rat brain and (*C* and *D*) adult mouse brain. GFP is visualized by anti-GFP staining. Confocal microscopy of triple immunostaining for GFP (green), cell cycle marker pH3 (blue), and neural progenitor marker nestin (red) demonstrates (*E*) no positive staining of pH3 in the graft. In nonpurified, predifferentiated mES transplants (*F*), large number of pH3-expressing cells could be detected. (*G*) Coronal section of mouse brain demonstrating typical appearance of a large tumor 4 wk after transplantation of nonpurified cells. (Scale bar, 100 μm.)

sorting the cultures were fixed and immunostained for the neuronal marker βIII-tubulin. We found that the GFP-expressing sorted cells efficiently differentiated into neurons (Fig. 3*C*). In summary, these experiments demonstrate that the miRNA-regulated system can be used to isolate differentiated progeny for molecular analysis and also be used to enrich viable neural progenitor cells.

Transplantation of FACS-Isolated Progenitors. A major issue that remains to solve when using pluripotent cells in grafting experiments, and for subsequent cell therapy, is to avoid transplanting immature cells that commonly contaminate predifferentiated cell suspensions. This contamination may lead to teratoma formation, aberrant overgrowth of the transplant or to rejection of the transplant through an immune-mediated reaction (6, 7, 15). Hence, by isolating and transplanting GFP-expressing mES.292Ts it may be possible to improve both survival and reduce tumor formation enabling studies to assess the grafting potential of pluripotent cells. To this end, we FACS-purified GFP-expressing mES.292T cells at day 8 of PA6-differentiation and transplanted the cells directly into the striatum of rodent brain. Four weeks after transplantation we found surviving grafts in six of eight animals. All of these transplants contained large number of cells that displayed mature neuronal morphologies as visualized by GFP expression (Fig. 4 *A–D*). In the surviving grafts, we detected no sign of proliferation in the striatum when using immunostaining for the pH3 (Fig. 4*E*) and detected only a limited number of cells expressing nestin (Fig. 4*E*). Only in one animal a transplant-derived tumor was detected and in this case outside the brain in close proximity to the skull. These results are encouraging when compared with the eight control animals that were transplanted with nonenriched cells that were otherwise treated identically. We did not detect a nonproliferating, neuron-rich transplant in any of the control animals (n = 8). Four of the animals displayed large overgrowths that contained large numbers of pH3-expressing cells (Fig. 4 *F* and *G*). Many of the pH3-expressing cells in nonsorted grafts were also positive for the neural progenitor marker nestin suggesting that it is not only pluripotent cells that divide but also immature neural progenitors (Fig. 4*F* and Fig. S6). The four other animals that received nonenriched cells displayed no signs of a surviving transplant. Similarly, previous experiences in the laboratory with predifferentiated nonenriched mES never gave rise to so many neuron-rich, tumor-free grafts as with miR-292 sorted cells (Fig. S7). Thus, we conclude that this approach reduces tumor formation and improves survival to a level that allows for consistent and reproducible grafting experiments.

Characterization of FACS-Sorted Transplants. The neuron-rich morphology, high survival-rate, and absence of overgrowth in the GFP-enriched mES.292T transplants allowed a detailed morphological characterization of the graft, which is normally not possible to perform when grafting mES. The GFP-enriched cells were transplanted into two rodent models of Parkinson's disease: neonatal rats with a unilateral 6-OHDA lesion (n = 4) and adult mice with a unilateral 6-OHDA lesion (n = 4).

Upon grafting in the neonatal rat model, the transplant could be also detected using the mouse-specific antibody M2M6, which largely overlapped with the GFP staining (Fig. S8). In the neonatal rat model we detected transplants with a dense core when staining for GFP (Fig. 4 *A* and *B*); but because GFP fills up the entire cell body, it was also possible to trace dense networks of GFP-positive processes throughout the striatum (Fig. S8). In addition to neurons we were also able to detect a large number of graft-derived astrocytes (Fig. S8).

The transplanted brains were then immunostained for tyrosine hydroxylase (TH) that marks dopaminergic neurons and also with an antibody recognizing 5-hydroxytryptamine (serotonin). The vast majority of transplanted GFP-expressing cells were in-

deed expressing TH with only a minority of the neurons expressing 5-HT (Fig. S9).

The transplants in adult mice were smaller when compared with the neonatal transplants. Still, GFP-staining revealed morphologies of mature neurons and it was also possible to trace processes within the striatum although the innervations from these transplants was less dense than when compared with neonatal transplants (Fig. 4 *C* and *D*). Finally, TH immunohistochemistry revealed that a smaller fraction of the GFP-expressing cells were TH-positive, suggesting differences in survival or differentiation of dopaminergic progenitors when transplanting into the adult vs. the neontal host (Fig. S9).

In summary, these results demonstrated that FACS enriched mES.292T cells survive transplantation, differentiate to mature neurons that extend long processes and display reduced rates of overgrowth when compared with nonenriched transplants.

Validation of microRNA-Regulated Vectors on iPS Cells. Pluripotent cells have recently been generated from fibroblasts and other somatic cells using over-expression of specific transcription factors (16, 17). These induced pluripotent stem (iPS) cells hold promise both for cell therapy and experimental studies. With this in mind, we tested whether LV.292T can be used on iPS cells. For this experiment we used the imO3 iPS-cell line that was generated using virus-free overexpression of the programming factors c-Myc, Klf4, Oct4, and Sox2 and the daughter cell line imO3c8 that has had the four factors removed using Cre-based excision (18). A previous report demonstrated that whereas imO3c8-cells, which no longer express the programming factors, efficiently differentiate into neurons, the parent cell line imO3 differentiates poorly (18).

We transduced imO3 and imO3c8 cells with LV.292T resulting in similar viral integrants and then differentiated the iPS cells toward neurons using the monolayer protocol and monitored GFP expression with time (Fig. 5 *A* and *B*). The imO3c8-line started to express GFP in a similar temporal manner as we previously found with mES-cells reaching high levels of GFP after 10 and 14 d of differentiation (Fig. 5 *B* and *C*). The appearance of GFP expression was associated with a down-regulation of Oct4 expression and it was also possible to detect large numbers of GFP-expressing βIII-tubulin–positive neurons (Fig. 5 *C* and *D*). In contrast, the imO3-line that maintain expression of the four transgenic reprogramming factors largely failed to down-regulate Oct4 and did not initiate GFP expression in substantial numbers of cells (Fig. 5 *B* and *C*). These results demonstrate that the LV.292T-vector can be used to monitor the differentiation capacity of iPS cells.

It is worth mentioning that we also found the LV.292T vector to be extremely useful to monitor expansion conditions for iPS-cells. iPS cells grown under nonoptimal conditions that led to partial spontaneous differentiation were easily detected by the high level GFP expression found in such cultures. Because different iPS cell lines can be difficult to maintain and require customized conditions, the LV.292T-vector may be a valuable tool for monitoring if iPS cells are grown under self-renewing conditions and may be used to assist optimization of culture conditions.

Validation of miRNA-Regulated Vectors on Human ES Cells. Finally, we wanted to validate whether the miRNA-regulated reporter system was also applicable to human pluripotent cells. In theory, miRNA-regulated vectors can be directly transferred between species because o the large degree of conservation of miRNAs. In particular, the murine miR-292 used in this study has a human homolog (miR-371) with a similar expression pattern and target sequence. After transducing the human ES cell line SA121 with LV.292T, no GFP expression was detected in hES colony cells, whereas the layer of irradiated fibroblast feeder cells displayed high-level GFP expression. However, with passaging, these GFP-expressing feeder cells were diluted and finally lost (Fig. 6*A*). In comparison, hES transduced with a control LV.GFP vector displayed high-level GFP in the undifferentiated ES cell colonies (Fig. 6 *A* and *B*).

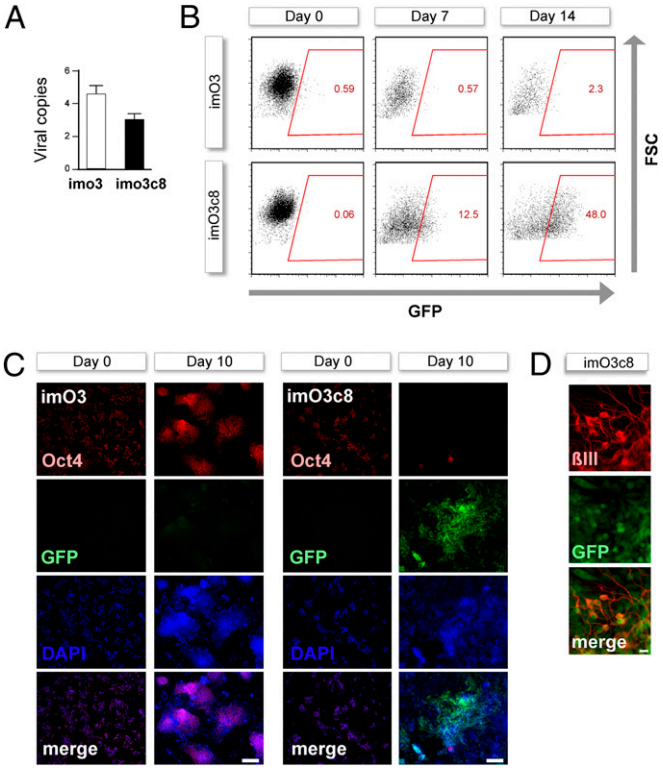

Fig. 5. LV.292T-vector system can be used to monitor differentiation of iPS cells. The iPS lines imO3, which constitutively express the reprogramming factors, and the imO3c8-cells, in which the reprogramming factors have been removed, were transduced with LV.292T and then differentiated toward a neural lineage using the monolayer protocol. (*A*) Quantification of viral copies/cell using quantitative PCR from genomic DNA of the cells analyzed in *B* and *C* (n = 3). (*B*) FACS analysis and (*C*) immunocytochemistry demonstrated that imO3c8 but not imO3-cells switch on GFP, and that this is correlated with down-regulation of Oct4 expression. (*D*) Fluorescence microscopy of GFP-expressing βIII-tubulin–positive neurons derived from imO3c8-cells differentiated for 10 d. Error bars represent SD. FSC, forward scatter. (Scale bar, *B*, 100 μm; *C*, 10 μm.)

We differentiated the LV.292T-transduced hES cells using a dual-inhibitor protocol recently described by Chambers et al. that results in a uniform neural induction (2). We monitored GFP expression as differentiation proceeded with fluorescent microscopy and FACS analysis. As with murine cells, we detected only negligible GFP expression at early time points. However, starting at day 10 of differentiation, the first GFP-expressing cells started to appear, reaching a maximum at 19 d of differentiation (Fig. 6 *C* and *D*).

We then applied a second differentiation protocol that proceeds via embryoid bodies and formation of neural rosettes (7). Also, with this protocol, GFP-expressing cells started to appear at approximately day 10. In this protocol, which gives rise to a heterogeneous population of cells, we were able to confirm that GFP-expressing cells colocalized with βIII-tubulin but did not colocalize with the pluripotency marker Oct4 (Fig. 6*E*).

In summary, these experiments demonstrate that the miR-292 system appears to be broadly applicable to different pluripotent cell lines. Importantly, transfer of the system from mouse to human cells can be easily achieved.

Discussion

In this study we used a miRNA-regulated lentiviral vector to visualize and segregate differentiated progeny in cultures of pluripo-

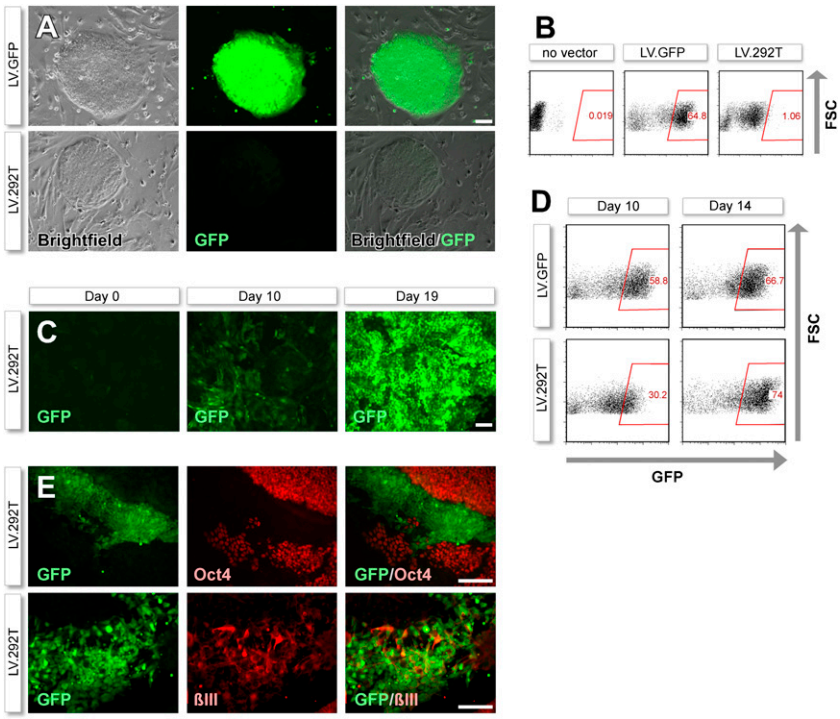

Fig. 6. LV.292T-vector system can be transferred to human ES cells. (*A*) Brightfield and fluorescence microscopy and (*B*) FACS analysis of live human ES cells transduced with either LV.GFP or LV.292T. (*C*) Fluorescence microscopy and (*D*) FACS analysis at different time points of human ES cells differentiated toward a neural lineage. (*E*) Double immunostaining for GFP (green) and Oct4 (red), and GFP (green) and βIII.tubulin (red), of human ES cells differentiated for 10 d. (Scale bar, 100 μm.)

tent cells differentiating toward the neural lineage. The main advantage of this strategy, when compared with related techniques such BAC transgenesis and knock-in reporters, is the simplicity. Key to the approach is the exploitation of the endogenous miRNA expression pattern that ensures proper transgene regulation. Because the system is based on lentiviral vectors, which are simple to use for genetic manipulations of various stem cell lines, it is possible to apply the technique to multiple cell lines in a short time frame. Importantly, we were easily able to transfer the system between murine ES cells, murine iPS cells, and human ES cells.

In this study, we focus on miR-292, which is specifically expressed in pluripotent cells. We found that our system allowed efficient removal of undifferentiated pluripotent cells using FACS sorting. In all of our experiments, we found that GFP expression appeared when expression of Oct4 was down-regulated, raising the possibility that Oct4 directly regulates miR-292 expression. In support of this notion, a recent genome-wide chromatin immunoprecipitation experiment identified a binding site for Oct4 in the promoter region for the miR-290-locus that encodes miR-292 (14).

When the GFP-enriched cells were transplanted, cells survived and continued to differentiate into mature neurons. We found that removing the undifferentiated cells reduced the formation of tumors and led to neuron-rich transplants displaying mature neuronal morphologies. Because FACS-sorting never leads to a completely pure population (our sorts were in the range of 95–98% purity), complete removal of tumors seems unlikely. Still, a reduction at the level described in this study will allow detailed experiments that have the potential to clarify optimal differentiation protocols and reveal the differentiation capacity of various pluripotent cell lines.

In conclusion, this study demonstrates the versatility and efficiency of miRNA-regulated lentiviral vectors to separate cell populations from differentiating pluripotent cultures. Although the full potential of this application remains to be explored, it has the necessary characteristics to be a widely used tool in stem cell biology. In this study we have used a vector with target sites for miR-292. Because this miRNA is specifically expressed in pluripotent cells, it was possible to visualize and segregate all differentiated progeny without selecting a specific population, and we provide ample evidence that this reporter accurately labels differentiated cells. Although excluding pluripotent cells using this strategy benefit of its simplicity, future experiments may require that more specific cell populations are isolated. With the growing literature of microRNA expression patterns during brain development, such experiments should be straightforward to perform, using lenitviral vectors incorporating target sequences for miRNAs with more specific expression patterns.

Materials and Methods

Lentiviral Vectors. A detailed description on how to generate lentivectors with miRNA-target sequences has been published elsewhere (11). The lentiviral vectors used in this study were third-generation lentiviral vectors containing a human UbiquitinC promoter (19). The target sequence for miR-292–3p is acactcaaaacctggcggcactt. Lentiviral vector stocks were produced as previously described (20). Lentiviral vectors were titrated by flow cytometry analysis and quantitative PCR analysis as previously described (21). The titers of the vectors used in this study were in the range of 5×10^8–2×10^9 TU/mL. An MOI of 50 was used for mES and hES, and an MOI of 10 was used for mNS. For transduction, vector stock was added to the medium, and 24 h later the vector-containing media was replaced and changed to fresh culture media.

Cell Culture. Murine NS cells were derived from E14 mouse ES cells and cultured as previously described (13). E14 mouse ES cells were maintained as previously described with minor modifications (5). Briefly, cells were expanded in DMEM (Gibco) supplemented with 10% FCS (BioSera), nonessential amino acids (Gibco), sodium puryvate (Gibco) glutamine (Sigma Aldrich), penicillin/streptomycin (Sigma Aldrich) and leukemia inhibitory factor (LIF) on gelatin-coated culture flasks (Nunc). Every second day the cells were passaged using trypsin and plated at a density of 4×10^4 cells/cm^2. Virus-free four-factor–derived mouse iPS-cells were maintained as previously described (18).

Monolayer differentiation was performed as previously described (5). Differentiation on PA6 stromal cells was carried out as previously described with minor modifications (3). One day before differentiation, PA6 cells were irradiated at 50 Gy and plated at a density to coat the culture flask. The following day, ES cells were added at a density of 60 cells/cm^2 in DMEM supplemented with 10% knock-out serum replacement (KSR, Gibco), nonessential amino acids, glutamine and penicillin/streptomycin. At day 8, the medium was replaced with N2B27 (StemCellSciences) for the remainder of the 14-d differentiation period.

The hES cell line SA121 (Cellartis; 46XY) was maintained as previously described with minor modifications (7). Briefly, ES cells were grown on a layer of murine embryonic fibroblasts, previously irradiated at 40 Gy, in knockout DMEM supplemented with 15% KSR, 5% human plasma protein (Bayer), 2 mM glutamax (Invitrogen), 1% nonessential amino acids (Invitrogen), 2β-mecaptoethanol (Invitrogen), penicillin/streptomycin (Sigma Aldrich), and 10 ng/mL basic fibroblast growth factor (bFGF; R&D). The ES cells were passaged every fourth day at a 1:3 split ratio using 0.05% trypsin.

Differentiation of human ES cells according to Chambers et al. was performed as described (2). Differentiation of hES via embryoid bodies was induced by changing the media to neural induction medium, which consists of DMEM:F12 (Gibco) and Neurobasal (Gibco) media at a 1:1 ratio supplemented with 2 mM glutamax (Invitrogen), 1× N2 (100× stock, Gibco), 1× B27 (50× stock, Gibco), and 100 ng/mL Noggin (R&D). After 1 d, cells were passaged en bloc (≈50–100 cells/cluster) and transferred to a nonadherent Petri dish (BD Falcon), where they were allowed to form embryoid bodies for 7 d when they where transferred to a PolyLysine laminin (Gibco)–coated dish. On the following day, when embryoid bodies had attached, the medium was changed to neural proliferation medium, which is similar to neural induction medium except that only half of the concentrations N2 and B27 are used.

All cells were fixed with 4% paraformaldehyde (VWR) in 0.1 M PBS for 15 min, followed by rinses in PBS. FACS sorting was performed as previously described (22). For quantitative immunofluorescent characterization, we plated cells immediately after FACS sorting. In brief, Shandon TPX filter cards (Thermo Scientific) were placed on Superfrost PLUS glass slides (Thermo Scientific) and attached to a funnel (Thermo Scientific). Filters were prerun with 100 μL PBS for 2 min at 1,000 rpm using a Cytospin (Thermo Scientific). A 250-μL volume of cell suspension was added and centrifuged for 4 min at 1,000 rpm.

Quantitative RT-PCR. Total RNA was isolated using the RNeasy Mini kit (Qiagen) according to the supplier's recommendations. A 500-ng quantity of RNA was used for the reverse transcription performed with random primers (Invitrogen) and SuperScriptIII (Invitrogen) according to the supplier's recommendations. SYBR green quantitative real-time PCR was performed with LightCycler 480 SYBR Green I Master (Roche) using standard procedures. Data were quantified using the ΔΔCt-method and normalized to GAPDH and β-actin expression. GAPDH-normalized data were very similar to actin data. Primers were designed using PrimerExpress software (Applied Biosystems). The efficiency of all primers was confirmed by performing reactions with serially diluted samples. The specificity was confirmed by analyzing the dissociation curve. Primer sequences were as follows: GAPDHFW: TCCATGACAACTTTGGCATTG; GAPDHREV: CAGTCTTCTGGGTGGCAGTGA; β-actinFW: CTAAGGCCAACCGTGAAAAGAT; β-actinREV: CACAGCCTGGATGGCTACGT; NanogFW: GCA AGC GGT GGC AGA AAA; NanogREV: GGT GCT GAG CCC TTC TGA ATC; Oct4FW: TGG CGT GGA GAC TTT GCA; Oct4REV: GAG GTT CCC TCT GAG TTG CTT TC; NestinFW: GACCACTTCCCTGATGATCCA: NestinREV: TCTAAAATAGAGTGGTGAGGGTTGAG; BLBPFW: GGGCGTGGGCTTTGC; BLPBREV: CTTCCTGACTGATAATCACAGTTGGT.

Animals. Neonatal rats and adult mice (Charles River) were used as recipients. All animal-related procedures were approved by and conducted in accordance with the committee for use of laboratory animals at Lund University. Neonatal stereotaxic procedures were performed as previously described (7). In brief, on postnatal day 1, rats were unilaterally injected with 6-OHDA into the right ventricle. On postnatal day 3, 1 μL cell suspension (100,000 cells/μL) was injected unilaterally into the dorsal lesioned striatum. Adult mice were injected with 6-OHDA into the right substantia nigra at 6–8 wk of age. Then, 4–6 wk later, 1 μL cell suspension (100,000 cells/μL) were unilaterally injected into the lesioned striatum. Four weeks after transplantation, animals were perfused with 4% PFA and the brains were postfixed, transferred to 25% sucrose, and sectioned into 35-μm-thick sections.

Immunohistochemistry. Similar procedures was followed for both fixed sections and cells, as published in detail elsewhere (23) Briefly, after preincubation for 1 h in blocking solution [5% normal serum and 0.25% Triton-X in 0.1 M potassium phosphate buffered saline (KPBS)], the primary antibody was diluted in the blocking solution and applied overnight at RT. Following rinses in KPBS, either biotinylated (Vector Labs) or fluorophore-conjugated secondary antibodies (Molecular Probes or Jackson Laboratories) were diluted in blocking solution and applied for 2 h. Biotinylated secondary antibodies were followed by 1-h incubation with fluorophore-conjugated streptavidin. Following fluorescent labeling, the free-floating sections were mounted on coated glass slides, and all sections and cells were cover-slipped with the anti-bleaching reagent PVA-DABCO.

Primary antibodies were diluted as follows: GFP (goat 1:500 or rabbit 1:20,000; both Abcam); M2 and M6 (mouse 1:50; Developmental Studies Hybridoma Bank), TH (mouse 1:4,000; Chemicon, or rabbit 1:1,000; Pelfreeze), βIII-tubulin (mouse 1:1,000; Promega), Oct4 (mouse 1:100; Santa Cruz), and pH3 (rabbit 1:200; Millipore). The dilution factors of the secondary antibodies were 1:500 (Molecular Probes) or 1:200 (Jackson Laboratories).

ACKNOWLEDGMENTS. We thank U. Jarl, A. Josefsson, C. Isaksson, A.-K. Oldén, Z. Ma, E. Ling, and B. Mattson for technical assistance, and K. Kaji for iPS cells. The hybridomas M2M6, developed by C. Lagenaur, were obtained from Developmental Studies Hybridoma Bank. This study was supported by grants from Parkinsonfonden (to J.J.), Hjärnfonden (to J.J.), Swedish Research Council (Grant 04X-2847 to A.B and M.P.), Knut and Alice Wallenberg Foundation (to A.B.), the EC 7th Framework program NeuroStemCell (Grant Agreement 22943 to A.B. and M.P.), and the Basal Ganglia Disorders Linnaeus Consortium supported by Vetenskapsrådet (to A.B., M.P., and J.J.).

1. Murry CE, Keller G (2008) Differentiation of embryonic stem cells to clinically relevant populations: Lessons from embryonic development. *Cell* 132:661–680.
2. Chambers SM, et al. (2009) Highly efficient neural conversion of human ES and iPS cells by dual inhibition of SMAD signaling. *Nat Biotechnol* 27:275–280.
3. Kawasaki H, et al. (2000) Induction of midbrain dopaminergic neurons from ES cells by stromal cell-derived inducing activity. *Neuron* 28:31–40.
4. Kim JH, et al. (2002) Dopamine neurons derived from embryonic stem cells function in an animal model of Parkinson's disease. *Nature* 418:50–56.
5. Ying QL, Stavridis M, Griffiths D, Li M, Smith A (2003) Conversion of embryonic stem cells into neuroectodermal precursors in adherent monoculture. *Nat Biotechnol* 21: 183–186.
6. Aubry L, et al. (2008) Striatal progenitors derived from human ES cells mature into DARPP32 neurons in vitro and in quinolinic acid-lesioned rats. *Proc Natl Acad Sci USA* 105:16707–16712.
7. Friling S, et al. (2009) Efficient production of mesencephalic dopamine neurons by Lmx1a expression in embryonic stem cells. *Proc Natl Acad Sci USA* 106:7613–7618.
8. Placantonakis DG, et al. (2009) BAC transgenesis in human embryonic stem cells as a novel tool to define the human neural lineage. *Stem Cells* 27:521–532.
9. Irion S, et al. (2007) Identification and targeting of the ROSA26 locus in human embryonic stem cells. *Nat Biotechnol* 25:1477–1482.
10. Bartel DP (2004) MicroRNAs: Genomics, biogenesis, mechanism, and function. *Cell* 116:281–297.
11. Brown BD, et al. (2007) Endogenous microRNA can be broadly exploited to regulate transgene expression according to tissue, lineage and differentiation state. *Nat Biotechnol* 25:1457–1467.
12. Brown BD, Venneri MA, Zingale A, Sergi Sergi L, Naldini L (2006) Endogenous microRNA regulation suppresses transgene expression in hematopoietic lineages and enables stable gene transfer. *Nat Med* 12:585–591.
13. Conti L, et al. (2005) Niche-independent symmetrical self-renewal of a mammalian tissue stem cell. *PLoS Biol*, 10.1371/journal.pbio.0030283.
14. Marson A, et al. (2008) Connecting microRNA genes to the core transcriptional regulatory circuitry of embryonic stem cells. *Cell* 134:521–533.
15. Miura K, et al. (2009) Variation in the safety of induced pluripotent stem cell lines. *Nat Biotechnol* 27:743–745.
16. Takahashi K, et al. (2007) Induction of pluripotent stem cells from adult human fibroblasts by defined factors. *Cell* 131:861–872.
17. Takahashi K, Yamanaka S (2006) Induction of pluripotent stem cells from mouse embryonic and adult fibroblast cultures by defined factors. *Cell* 126:663–676.
18. Kaji K, et al. (2009) Virus-free induction of pluripotency and subsequent excision of reprogramming factors. *Nature* 458:771–775.
19. Lois C, Hong EJ, Pease S, Brown EJ, Baltimore D (2002) Germline transmission and tissue-specific expression of transgenes delivered by lentiviral vectors. *Science* 295: 868–872.
20. Zufferey R, Nagy D, Mandel RJ, Naldini L, Trono D (1997) Multiply attenuated lentiviral vector achieves efficient gene delivery in vivo. *Nat Biotechnol* 15:871–875.
21. Georgievska B, et al. (2004) Regulated delivery of glial cell line-derived neurotrophic factor into rat striatum, using a tetracycline-dependent lentiviral vector. *Hum Gene Ther* 15:934–944.
22. Jönsson ME, Ono Y, Björklund A, Thompson LH (2009) Identification of transplantable dopamine neuron precursors at different stages of midbrain neurogenesis. *Exp Neurol* 219:341–354.
23. Thompson L, Barraud P, Andersson E, Kirik D, Björklund A (2005) Identification of dopaminergic neurons of nigral and ventral tegmental area subtypes in grafts of fetal ventral mesencephalon based on cell morphology, protein expression, and efferent projections. *J Neurosci* 25:6467–6477.